Effect of Subsequent Drying and Wetting on the Small Strain Shear Modulus of Unsaturated Soils

A. Khosravi, S. Ghadirian, J. S. McCartney

Abstract—Evaluation of the seismic-induced settlement of an unsaturated soil layer depends on several variables, among which the small strain shear modulus, G_{max}, and soil's state of stress have been demonstrated to be of particular significance. Recent interpretation of trends in G_{max} revealed considerable effects of the degree of saturation and hydraulic hysteresis on the shear stiffness of soils in unsaturated states. Accordingly, the soil layer is expected to experience different settlement behaviors depending on the soil saturation and seasonal weathering conditions. In this study, a semi-empirical formulation was adapted to extend an existing G_{max} model to infer hysteretic effects along different paths of the SWRC including scanning curves. The suitability of the proposed approach is validated against experimental results from a suction-controlled resonant column test and from data reported in literature. The model was observed to follow the experimental data along different paths of the SWRC, and showed a slight hysteresis in shear modulus along the scanning curves.

Keywords—Hydraulic hysteresis, Scanning path, Small strain shear modulus, Unsaturated soil.

I. INTRODUCTION

DIFFERENT methods have been proposed to analyze the behavior of soils under cyclic loading and their seismically-induced settlements such as equivalent linear [19] and non-linear [9], [11], [14], [18] analyses. In these methods, the analysis is performed using some relevant terms affecting the settlement behavior such as damping ratio (constant or function of cyclic shear strain), effective stress, pore water pressure, small strain shear modulus, G_{max} (constant or function of effective stress), and shear modulus reduction function (G/G_{max} as a function of cyclic shear strain), mostly developed for soils in dry and saturated states. However, it has been recognized for some time now that the seismic response of soil at a particular site is dramatically affected by the degree of saturation of soil, S_r, and its unsaturated stress state variables [1], [5].

Reference [1] performed a series of physical model centrifuge tests to simulate ground motions and studied the settlement behavior of an unsaturated layer of sand during seismic loading. The seismic load in this study was provided using an electrohydraulic shaking table mounted on the platform of centrifuge, and the Steady-State Infiltration Method [15] was used to provide uniform target suction

A. Khosravi and S. Ghadirian are the Civil Engineering Department, Sharif University of technology, Tehran, Iran (corresponding author, phone: +98-21-66164208; e-mail: khosravi@ sharif.edu, Saharghadiriaan@gmail.com).

J. S. McCartney is with the Department of Structural Engineering, University of California, San Diego, La Jolla, CA 92093-0085 (e-mail: mccartney@eng.ucsd.edu).

through the height of the sand layer. Results of their study revealed the significant effect of degree of saturation on the soil settlement behavior during seismic loading. The soil settlement-degree of saturation curve showed an initial decrease in settlement during drying to a critical point at a S_r value of approximately 0.7, followed by an increasing trend. It is interesting to note that the trend for the soil settlement was observed to be consistent with the shape of the G_{max}-S_r curve during the drying path.
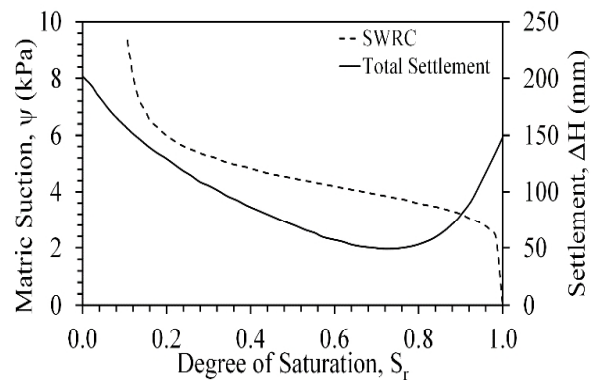

Fig. 1 Matric suction and settlement variation with S_r

From the results of the centrifuge tests, [1] proposed and verified an empirical methodology to predict the earthquake induced settlement of a free field unsaturated sand layer. The new methodology incorporated recent advances in the definition of the effective stress and stiffness in unsaturated soils, and soil-water retention curve parameters into existing approaches originally developed for saturated soils. In particular, the small strain shear modulus was defined using an effective stress-based approach proposed by [5] as:

$$G_{max} = \frac{A}{0.3 + 0.7e^2} p'^{m} \tag{1}$$

where, A and n are fitting parameters, e is the initial void ratio and p' is the mean effective stress which was defined using the concept of suction stress proposed by [13]. Equation (1) was observed to provide a good prediction of the small strain shear modulus for unsaturated sands. However, it only considered the role of matric suction and net stress on G_{max} measurements along the drying path of the SWRC.

Later studies by [8], [16], [22] showed the importance of concurrent consideration of S_r and ψ in interpreting G_{max} measurements during hydraulic hysteresis, especially when testing fine graded materials, and some correlations between

the small strain shear modulus and degree of saturation were developed from the results of element scale tests. These correlations improved the prediction of G_{max} during hydraulic hysteresis. However, they failed to predict the values of G_{max} along the scanning curves of the SWRC. Fluctuating field conditions may result in the occurrence of unsaturated/ saturated conditions in the soil layers. This may correspond to wetting and drying on scanning curves between the primary drying and wetting paths of the SWRC.

In this paper, a methodology is proposed to capture changes in G_{max} magnitude along different paths of the SWRC including drying/scanning/rewetting paths. In this regard, the proposed equation for G_{max} by [8] is extended by implementing an empirical relationship that predicts S_r values along the scanning paths of the SWRC based on [17] approach. The suitability of the proposed methodology is assessed through comparison with experimental results from a suction-controlled resonant column test and from data reported in literature.

II. A METHODOLOGY FOR PREDICTING SMALL STRAIN SHEAR MODULUS ALONG THE SCANNING PATHS OF THE SWRC

Reference [8] adapted the G_{max} relationship proposed by [3] for saturated soils to consider the role of matric suction and hydraulic hysteresis on G_{max} of low plasticity unsaturated soils. This formulation incorporated two terms including plastic changes in volume and changes in degree of saturation to consider the effect of hydro-mechanical coupling in evaluation of G_{max} as:

$$G_{max} = AP_a \left[\frac{p_c{'}_0}{p_n} \exp\left(\frac{\Delta e^p}{\lambda - \kappa}\right) \right]^K \left[\frac{p_n}{p'} \exp\left(b[S_{e0} - S_e]\right) \right]^{K'} \left(\frac{p'}{P_a}\right)^n \quad (2)$$

where A and n are effective stress dependency parameters, P_a is the atmospheric pressure, $p_c{'}_0$ is the initial mean apparent pre-consolidation stress, p_n is the net stress, p' is the mean effective stress defined using the suction stress concept as $p' = p_n + \psi \times S_e$, Δe^p is a plastic change in void ratio, λ and κ are the slopes of the isotropic compression and unloading curves, K' and K are hardening parameters, b is the double hardening parameter referring to the effects of changes in soil saturation, and S_e and S_{e0} are the values of effective saturation at current and initial conditions, respectively. The value of effective saturation, S_e, was defined using the SWRC model of [20], which allows the prediction of degree of saturation and hydraulic behavior along the main drying and wetting paths of SWRC. However, it fails to predict the degree of saturation along scanning drying and wetting curves.

In this study, an empirical approach proposed by [17] was implemented in (2) to capture the variations of S_e along different paths of the SWRC. [17] used two parameters, the air saturation, S_a, and the apparent saturation, S_{app}, to estimate the amount of trapped air during wetting. S_{app} was used to consider the air entrapment along the scanning curves and is obtained using the following equation:

$$S_{app} = \frac{\left[S_{van}^p - S_{van}^p(\psi_{i-1}) \right](S_i - S_{i-1})}{\left[S_{van}^p(\psi_i) - S_{van}^p(\psi_{i-1}) \right]} + S_{i-1} \quad (3)$$

where p is an index indicating whether a drying or wetting scanning path is considered. S_{van}^p is the effective saturation of the main path. $S_{van}^p(\psi_i)$ and $S_{van}^p(\psi_{i-1})$ are the values of effective saturation of the most recent and previous reversal points, calculated using the van Genuchten equation, and S_i and S_{i-1} are the apparent saturations of the most recent and previous reversal points, respectively. Fig. 2 shows a hypothetical SWRC and different paths of drying, wetting and scanning to clarify this designation. For a path like 1-2 which lies on the main drying curve, the most recent reversal point would be point 1 with the values of $(S_i, \psi_i) = (1,0)$, and the previous reversal point has the values of $(S_{i-1}, \psi_{i-1}) = (0, \infty)$. Path 2-3 is a scanning wetting path with the values of (S_i, ψ_i) corresponding to point 2 and (S_{i-1}, ψ_{i-1}) corresponding to the previous point 1. Path 3-4 is a scanning drying path with the most recent and previous reversal points of 3 and 2, respectively. The same manner can be followed through any other path to define the reversal points in calculations.
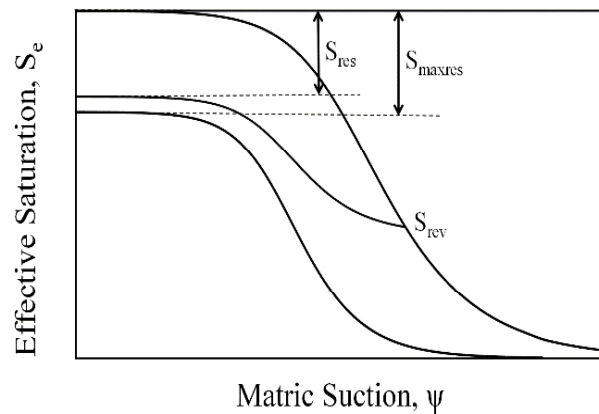

Fig. 2 Theoretical scanning loops of a hypothetical apparent saturation curve

Now, with the value of apparent saturation (3), the air saturation, S_a at any intermediate point along the scanning wetting paths is obtained by linearly interpolating air saturations between the end points of primary wetting curves and using the maximum trapped saturation as follows [12]:

$$S_a = S_{res}\left(\frac{S_{app} - S_{rev}}{1 - S_{rev}}\right) \quad (4)$$

where, S_{app} is the apparent saturation, S_{rev} is the effective saturation at the reversal point from the main drying curve to a primary scanning wetting path (Fig. 3), and S_{res} is the effective residual saturation of trapped air along the primary scanning path given by the following equations [17]:

$$S_{res} = \frac{1 - S_{rev}}{1 + R\left(1 - S_{rev}\right)} \quad (5)$$

in which

$$R = \frac{1}{S_{max\,res}} - 1 \quad (6)$$

With the values of apparent saturation (3) and air saturation, the effective saturation of water is obtained as:
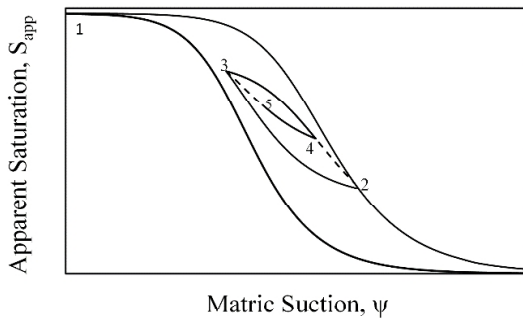
$$S_e = S_{app} - S_a \quad (7)$$

Fig. 3 Different parameters involved in air entrapment determination

By implementing (7) into the model proposed by [8], G_{max} values along main drying and wetting curves as well as the scanning paths of the SWRC can be obtained. Fig. 4 shows the results of a parametric evaluation to highlight the functional behavior of the extended G_{max} model along the scanning loops of the SWRC during hydraulic hysteresis. In this regard, a hypothetical soil specimen subjected to an initial value of mean net stress of p_n=100 is used and the effect of two hardening parameters, b in Fig. 4 (a) and K' in Fig. 4 (b) are discussed.

The presented trends in G_{max} imply that an increase in K' leads to a greater impact of hydraulic hysteresis on G_{max} values while imposing greater values of b results in steeper rate of change in G_{max} along the scanning path. Results also indicate that under small changes in matric suction along the scanning curves of the SWRC, the hysteresis effects are negligible and a unique form of SWRC can be assumed for the material.

III. EXPERIMENTAL VALIDATION

The methodology presented in this study for the G_{max} values along different paths of the SWRC was validated against a set of G_{max} values obtained from a series of resonant column tests on a specimen of silt, obtained from Bonny dam near the Colorado-Kansas Border. The tests were performed using a fixed-free resonant column test device modified with a feedback-controlled flow pump and the axis translation technique to reach different equilibrium values of ψ and S_e. The soil has a specific gravity of 2.6, plasticity index of 4 and is classified as ML according to the Unified Soil Classification System (USCS). The soil specimen has a diameter of 36mm,

height of 72mm, statically compacted at an initial water content of 14% to reach a dry density of 15.09 kN/m³.
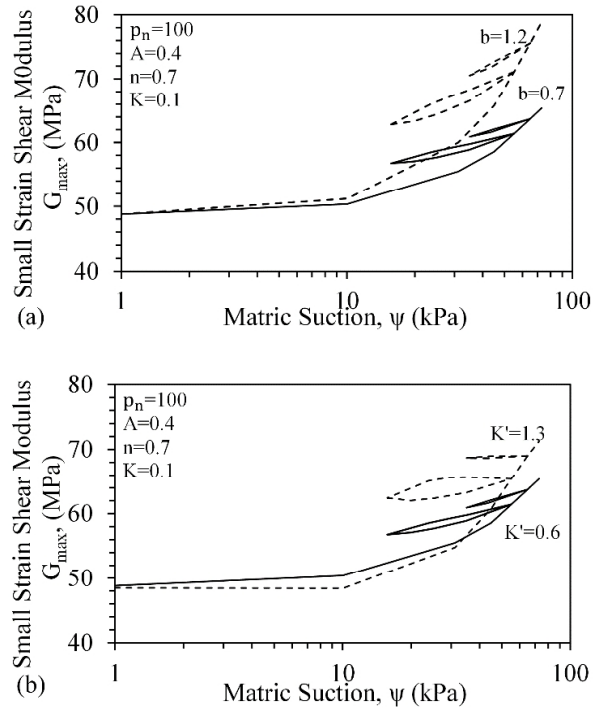

Fig. 4 Parametric evaluation of the effects of hardening parameters on G_{max} during successive wetting-drying cycles (a) impact of hardening parameter b on G_{max} (b) impact of the hardening parameter K' on G_{max}

In this experimental study, after placement of the soil specimen within the test setup and achieving the full saturation using the backpressure technique, the soil specimen was initially dried to a suction value of 31 kPa along the main drying path of the SWRC under a mean net stress of 70 kPa. After that, the direction of the flow pump was reversed and the applied suction was decreased in stages to a value of 21 kPa to produce the first scanning curve of the test. At each point of suction equilibrium, a resonant column test was performed and the value of G_{max} of the soil specimens was measured. The specimen was then re-dried and a similar procedure was followed at suction values of 41 and 61 kPa for simulating three full cycles of drying and wetting. The testing device and procedure for this device are described in detail by [6], [7].

The SWRCs of the tested specimen are shown in Fig. 5 (a) and the variations of G_{max} measured after reaching matric suction equilibrium are presented in Fig. 5 (b). Fig. 5 also shows the van Genuchten [20] SWRC model, fitted to the experimental data over the range of suction imposed to the specimen (Fig. 5 (a)). The SWRC model parameters were obtained by fitting the best-fitted curve to the experimental results along different path of the SWRC. The Results of shear modulus at small strain presented in this figure revealed a slight hysteresis in the G_{max} measurements along the scanning curves of the SWRC, with a larger loop along the second loop

where more significant changes in S_r happened with changing matric suction. However, in both cases, the value of G_{max} was recovered once the main drying path was reached. Fig. 5 (b) also shows comparisons between the experimental G_{max} data and the model for different paths as a function of ψ. The model parameters are presented in Table I. As listed in this table, the parameters required to predict the evolution of G_{max} along different paths of the SWRC include the hardening parameters (K, K', b), the parameters describe the slope of virgin compression and unloading curves (κ, λ), and the effective stress dependency parameters (A, n).
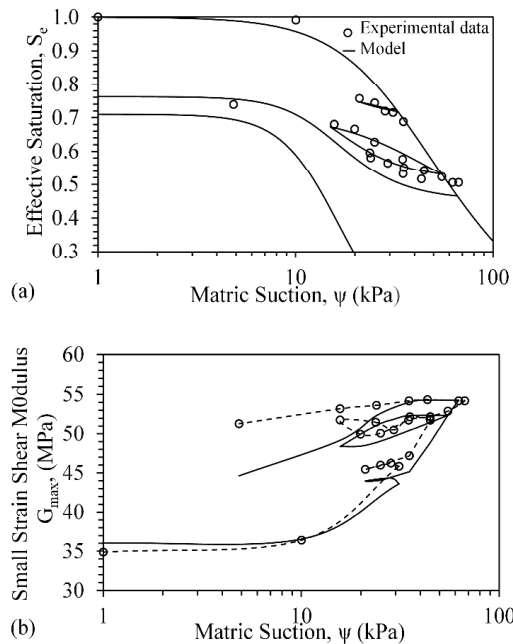

(a)

(b)

Fig. 5 Comparison of the data obtained from the resonant column results with the proposed methodology. (a) SWRC (b) G_{max}

TABLE I
G_{MAX} EQUATION PARAMETERS

A	0.41
n	0.68
K	0.05
K'	0.9
b	1.06
λ	0.15
κ	0.00002
p_n (kPa)	70 kPa
$p_c'_0$ (kPa)	720 kPa

In the current study, the values of $p_c'_0$ and b were obtained from the results of a series of isotropic compression tests on specimens subjected to different suction values [10], K was defined using empirical guidance from [2], A and n were defined by fitting a curve to the values of G_{max} measured under saturated conditions (zero suction) and K' was obtained from the G_{max} measurements at different equilibrium suction values along the drying path using least squares minimization. Plastic changes due to suction change were also considered zero in

(2). Similar values were used by [10] for the specimens with similar characteristics and dry densities. With the values presented in Table I, the values of G_{max} predicted using the proposed methodology are in good qualitative and quantitative agreement with the experimental data. The greatest discrepancy between the experimental data and the model occurs during wetting for the suctions lower than 20 kPa.

IV. LITERATURE DATA ANALYSIS

In order to further examine the application of the new model for small stain shear modulus of unsaturated soils along the scanning paths of the SWRC, the model was fit to G_{max} values reported in the literature. Figs. 6 and 7 present experimental SWRCs and G_{max} data for SP-SC [4], and MH [21], respectively. Characteristics of each soil are presented in Table II.

TABLE II
SOIL PROPERTIES

Literature data	Soil type	G_s	w_l (%)	w_p (%)	PI	Soil classification
[4]	Silty Sand	2.7	25.5	32.5	10	SP-SC
[21]	Po Silt	2.76	50.4	-	17.9	Inorganic Silt

A. G_{max} Data for SP-SC [4]

In this study, the values of G_{max} were measured on a specimen prepared at initial void ratio of 0.4 and dry density of 18.9 kN/m^3. The tests were performed using the bender element technique under an initial mean net stress of 50 kPa along two successive wetting and drying cycles (Fig. 6). The SWRC measurements and their corresponding G_{max} data are illustrated by the scatter in Figs. 6 (a) and (b), respectively. The experimental results in this figure are presented with the data points, while the lines show the predictions.

TABLE III
G_{MAX} EQUATION PARAMETERS

Equation parameters	Literature data	
	[4]	[21]
A	3.6	1.35
n	1.1	0.55
K	0	0.18
K'	1	0.9
b	2.8	7
λ	-	0.06
κ	-	0.018
p_n (kPa)	50	200
$p_c'_0$ (kPa)	720	510

In this study, the van Genuchten parameters, α and N, along the main drying path of the SWRC were obtained using the SWRC data reported in literature as shown in Fig. 6 (a). Other parameters including the values of α and N for the main wetting path were obtained by fitting the best-fitted curve to the experimental scanning curves. The initial value of $p_c'_0$ were not reported for the tested soil in this studies. So this variable was assumed and the parameters A, n, K, K' and b were found by fitting the model to the G_{max} data for unsaturated conditions. Plastic changes due to hydraulic

loading (suction change) were also ignored. With these parameters, the model was compared against the trends in G_{max} with ψ along different paths of the SWRC (Fig. 6 (b)). As presented in this figure, for the particular fitting values presented in Table III, a good consistency between the predicted G_{max} values with those measured experimentally is observed.
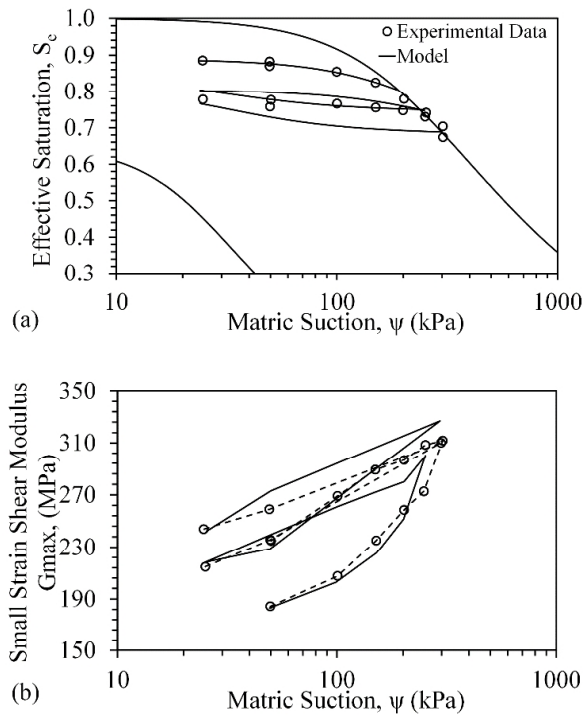

(a)

(b)

Fig. 6 Comparison of the data obtanid from [4] with the proposed methodology (a) SWRC (b) G_{max}

B. G_{max} Data for MH [21]

The SWRC measurements and the G_{max} values obtained from a series of triaxial and resonant column (RC) tests performed by [21] are presented in Figs. 7 (a) and (b), respectively. The results were performed on specimens of a silt used for the construction of embankments on the Po river in Italy, subjected to a mean net stress of 200 kPa. The RC test includes an initial compression stage at a suction of 400 kPa, followed by subsequent wetting and drying cycles between the suction values of 400 and 100 kPa [21]. Due to lack of data on the soil degree of saturation and compression curve, the model parameters were treated as fitting parameters and were defined by fitting the model to the data reported in this study (Table III).

A comparison between the predicted values of G_{max} and those measured experimentally indicates that the model provides reasonable prediction of the variations in G_{max} during the first loop of scanning. Results indicated a greater discrepancy between the data and the model, especially along the second path of the scanning curves. Better experimental SWRC measurements would probably result in better prediction of the S_e values along the scanning curves and their

corresponding G_{max} measurements.
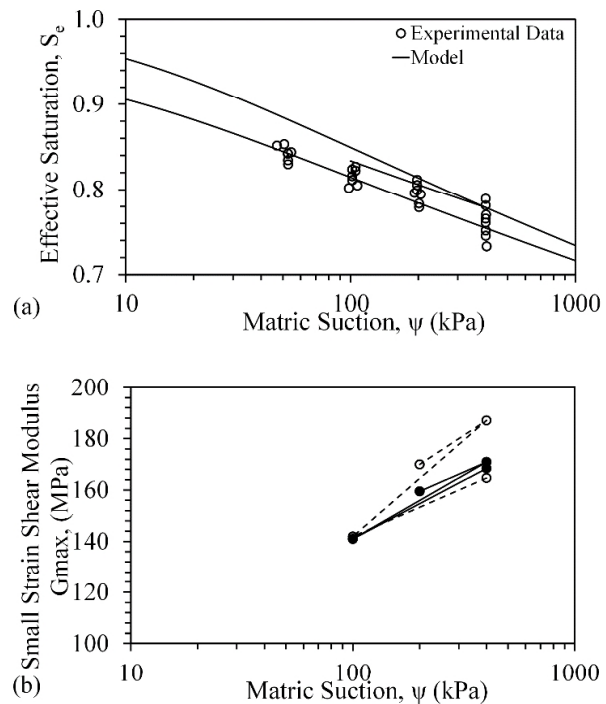

(a)

(b)

Fig. 7 Comparison of the data obtained from [21] with the proposed methodology (a) SWRC (b) G_{max}

V.CONCLUSION

A new methodology was presented in this study to infer the effects of the soil's degree of saturation and hydraulic hysteresis on the seismic response of unsaturated soil. The proposed methodology incorporates an empirical approach to define the characteristic relationships between the degree of saturation and matric suction to simulate the variations of G_{max} along the main drying and wetting paths of the SWRC as well as the scanning curves.

The validity of the model was investigated through comparison with experimental results from an independent experimental program, using a modified resonant column test device. For a mean net stress of 70 kPa, the small-strain shear modulus of statically-compacted Bonny silt was found to vary from 36 to 55 MPa for matric suctions ranging from 1 to 70 kPa (degrees of saturation from 1.00 to 0.48). The shear modulus of the soil was found to be greater upon re-wetting of the soil, a behavior which is attributed to the hardening caused by soil drying. The results also showed a slight hysteresis in the G_{max} measurements along the scanning curves of the SWRC. Using the model parameters defined through definition of the SWRC and compression curves, and through parameter fitting to the soil, the model used for the hysteretic SWRC was found to integrate well with the constitutive relationships to represent the change in G_{max} along different paths of the SWRC.

For further examination of the application of the new methodology for the small stain shear modulus of unsaturated

soils, the model was fit to G_{max} values reported in the literature along the main drying and scanning paths of the SWRC. The proposed methodology was found to fit well the trends in G_{max} values. Future testing on soils of different types and densities is recommended to investigate if the proposed methodology can be more broadly used to characterize the G_{max} behavior of unsaturated soils during hydro-mechanical loading.

REFERENCES

[1] Ghayoomi, M., McCartney, J. S., and Ko, H.-Y. (2013). "Empirical methodology to estimate seismically induced settlement of partially saturated sand." ASCE, Journal of Geotechnical and Geoenvironmental Engineering. 139(3), 367-376.
[2] Hardin, B.O. (1978). "The nature of stress stain behavior of soils." Earthquake Engineering and Soil Dynamics. 1, 3–90.
[3] Hardin, B.O. (1978). "The nature of stress-strain behavior of soils." Proceedings of Earthquake Engineering and Soil Dynamics, ASCE Pasadena, California, 1(3-89).
[4] Heitor, A., Indraratna, B., and Rujikiatkamjorn, C. (2014). "Aspects related to the small strain shear modulus behaviour of compacted soils subjected to wetting and drying." Proceedings of the 2014 Geo-congress: Geo-characterization and Modelling for sustainability, Atlanta, pp. 1433-1442.
[5] Khosravi, A., Ghayoomi, M., McCartney, J.S. and Ko, H.Y. (2010). "Impact of effective stress on the dynamic shear modulus of unsaturated sand." GeoFlorida 2010, West Palm Beach, Florida, USA. Feb. 20-24.
[6] Khosravi, A. (2011). "Small strain shear modulus of unsaturated, compacted soils during hydraulic hysteresis." Ph.D. diss., Boulder, Colorado: University of Colorado at Boulder.
[7] Khosravi, A., and McCartney, J.S. (2011). "Suction-controlled resonant column test for unsaturated soils." ASTM Geotech. Test. J., 34(6), 1-10.
[8] Khosravi, A. and McCartney, J.S. (2012). "Impact of hydraulic hysteresis on the Small-Strain shear modulus of low plasticity soils." ASCE, Journal of Geotechnical and Geoenvironmental Engineering, 138(11), 1326-1333.
[9] Khosravi, M., Tamura, S., Boulanger, R. W., Wilson, D. W., Olgun, C. G., Rayamajhi, D., Wang, Y., (2015). "Dynamic centrifuge tests on soft clay reinforced by soil-cement grids." IFCEE 2015, ASCE, Reston, VA, 2349-2358.
[10] Khosravi, A., Salam, S., McCartney, J. S., Dadashi, A. (2016). "Suction-induced hardening effects on the shear modulus of unsaturated silt." International Journal of Geomechanics, 10.1061/(ASCE) GM.1943-5622.0000614.
[11] Kramer, S.L. (1996). "Geotechnical earthquake engineering", Prentice Hall, New Jersey.
[12] Land, C.S. (1968). "Calculation of imbibition relative permeability for two and three-phase flow from rock properties." Soc. Pet. Eng. J, -8, 149-156.
[13] Lu N. and Likos W.J. (2006). "Suction stress characteristic curve for unsaturated soil." ASCE, Journal of Geotechnical and Geoenvironmental Engineering, 132(2), 131-142.
[14] Martin, G.R., Finn W.D.L., and Seed H. B. (1975). "Fundamentals of liquefaction under cyclic loading", Journal of Geotechnical Engineering Devision, ASCE, 101(5), 423-438.
[15] McCartney, J.S. and Zornberg, J.G. (2010). "Centrifuge permeameter for unsaturated soils. II: Measurement of the hydraulic characteristicsof an unsaturated clay." ASCE, Journal of Geotechnical and Geoenvironmental Engineering, 136(8), 1064-1076.
[16] Ng, C.W.W., Yung, S.Y. (2008). "Determination of the anisotropic shear stiffness of an unsaturated decomposed soil." Geotechnique, 58(1), 23–35.
[17] Parker, J.C., and Lenhard, R.J. (1987). "A model for hysteretic constitutive relations governing multiphase flow. 1: Saturation–pressure relations." Water Resources Research, 2312, 2187–2196.
[18] Rayamajhi, D., Tamura, S., Khosravi, M., Boulanger, R.W., Wilson, D., Ashford, S.A., and Olgun, C.G., (2015). "Dynamic Centrifuge Tests to Evaluate Reinforcing Mechanisms of Soil-Cement Columns in Liquefiable Sand." Journal of Geotechnical and Geoenvironmental Engineering, 140(3), 04015015-1.
[19] Seed, H.B., and Idriss, I.M. (1971). "Simplified procedure for evaluating soil liquefaction potential." J. Soil Mechanics Found. Div., ASCE, 97(9), 1249-1274.
[20] van Genuchten, M.T. (1980). "A closed-form equation for predicting the hydraulic conductivity of unsaturated soils." Soil Sci. Soc. Am. J., 44, 892–98.
[21] Vassallo, R., Mancuso, C., and Vinale, F. (2007a). "Effects of net stress and suction history on the small strain stiffness of a compacted clayey silt." Can. Geotech. J., 44(4), 447–462.
[22] Wong, K.S., Masin, D., and Ng, C.W.W. (2014). "Modelling of shear stiffness of unsaturated fine grained soils at very small strains". Computers and Geotechnics, 56, 28–39.